# Shape Matters: Corolla Curvature Improves Nectary Discovery in the Hawkmoth *Manduca sexta*

Eric Octavio Campos

A thesis

submitted in partial fulfillment of the

requirements for the degree of

Master of Science

University of Washington

2016

Committee:

H.D. 'Toby' Bradshaw

Thomas L. Daniel

Janneke Hille Ris Lambers

Program Authorized to Offer Degree:

Biology

University of Washington

**Abstract**

Shape Matters: Corolla Curvature Improves Nectary Discovery in the Hawkmoth *Manduca sexta*

Eric Octavio Campos

Co-Chairs of the Supervisory Committee:

Professor H.D. 'Toby' Bradshaw
Department of Biology

Professor Thomas L. Daniel
Department of Biology

I measured the effects of variation in corolla curvature and nectary aperture radius on pollinator foraging ability using the hawkmoth *Manduca sexta* and 3D-printed artificial flowers whose shapes were mathematically specified. In dimorphic arrays containing trumpet-shaped flowers and flat-disk flowers, hawkmoths were able to empty the nectaries of significantly more trumpet-shaped flowers regardless of nectary aperture size. Interestingly, trumpet-shaped flowers needed to deviate only slightly from the flat-disk morphotype in order to significantly increase hawkmoth foraging ability. Whole-flower three-dimensional shape, particularly corolla curvature, has the potential to act as a mechanical guide for *Manduca sexta*, further implicating direct flower-proboscis contact as an important contributor to foraging success during flower handling in hawkmoths.

# TABLE OF CONTENTS

# LIST OF FIGURES

Page



# LIST OF TABLES

Page

## Introduction

Many animals consume floral nectar as a primary means of meeting their energetic requirements (Kingsolver & Daniel 1995). Nectar feeding presents an interesting sensorimotor challenge for hovering animals, as they must modulate their aerodynamic forces to precisely position their feeding apparatus in the nectary of a flower that could potentially be swaying in the breeze generated by their flapping wings or by external winds. This mode of flight is metabolically demanding (Vogel 1994; Norberg 1990), making nectar discovery ability all the more important for hovering nectarivores.

Floral guides may aid the process of nectarivory by obligate hovering species. A guide is any phenotypic feature of a flower that acts as a cue to assist animals in finding the floral reward, nectar or otherwise (Sprengel 1793; Sprengel 1996). Floral guides are commonly thought of as visual stimuli (Medel et al. 2003), but the concept can be expanded to include stimuli that could be perceived by other sensory modalities such as chemical (Riffel et al. 2009a) and mechanical sensory pathways (Kevan & Lane 1985; Krenn 1998). Indeed, it has become increasingly evident that pollinators make use of multiple sensory modalities during the foraging process (Goyret & Raguso 2006; Goyret & Kelber 2011). Non-visual sensory information may be particularly critical for nocturnal and crepuscular animals, as they deal with reduced light levels compared to diurnal species. Despite such visual challenges, nocturnal and crepuscular animals effectively forage on night-blooming flowers and are important contributors to the pollination of various angiosperm species (Dar, Arizmendi, & Valiente-Banuet 2006; Groman & Pellmyr 1999; Goyret & Raguso 2006).

The hawkmoth *Manduca sexta* (Fig. 1) is a crepuscular pollinator that has an extensive history as a model organism in laboratory and field studies of pollination. It is also noted for its ability to track flower motion while hovering in mid air (Sprayberry & Daniel 2007). Although *M. sexta* sometimes lands on a flower during foraging, it also has the ability to feed by hovering a short distance from a flower, making contact only with its uncurled proboscis (Brantjes & Bos 1980; Raguso & Willis 2002). Previous research has shown that *M. sexta* is able to use both visual and mechanical floral guides during flower handling to aid in nectar discovery: experiments with flat-disk artificial flowers have shown that *M. sexta* preferentially probes with its proboscis at light-coloured areas of a flower, regardless of whether the nectary is present at those locations (Goyret 2010). In addition, groove-like features on a flower's surface may effectively guide the movement of the proboscis along the direction of the grooves (Goyret & Raguso 2006; Goyret 2010).

Recent results by others suggest that foraging by *M. sexta* is under multimodal sensory control, with different sensory modalities, or combinations of them, being important at different stages of the foraging process, depending on a moth's distance from a food source. For example, at large distances, a moth uses olfaction to orient toward a group of flowers (Brantjes 1978). At intermediate distances, the approach to a group of flowers is guided by either olfaction or vision, while extension of the proboscis requires that appropriate olfactory and visual stimuli be present simultaneously (Goyret & Raguso 2006). Once a moth has selected an individual flower, initial placement of the proboscis on the flower is visually guided, with light-colored regions being preferred over dark regions (Goyret 2010). Finally, when the proboscis is in contact with the

Figure 1. *Manduca sexta*, the pollinator used in this study, probing a flower with its proboscis. Photo by Armin Hinterwirth.

flower, mechanoreception through the proboscis ultimately is used to locate the nectar source (Goyret & Raguso 2006, Goyret 2010).

It is possible that corolla grooves are not the only mechanical stimuli used by moths during flower handling. Goyret and Raguso (2006) discussed the possibility that the trumpet-like shape of *Datura* flowers, from which *M. sexta* feeds in nature, may allow for more effective handling by moths in comparison with flat disks of the same diameter, but did not manipulate corolla shape in their study. Indeed, the stereotypical hawkmoth-pollinated flower is deemed to have a funnelform, tubular corolla (Fægri & van der Pijl 1966, Proctor et al 1996). *Datura*, *Petunia*, and *Nicotiana* (tobacco) flowers are a few examples of such funnelform hawkmoth-pollinated flowers.

Here, we test the hypothesis that the trumpet-shaped curvature associated with hawkmoth-pollinated flowers can act as a mechanical floral guide. This was motivated by our initial intuition that, if crepuscular hawkmoths "feel" their way into a flower's nectary with the proboscis, a flat-disk flower would provide no reliable tactile cues as to the location of the nectary, making it more likely that a moth would abandon a visit before the nectary is located. In contrast, the surface of a trumpet-shaped flower slopes toward the nectary and could passively guide the proboscis to the nectary regardless of where the proboscis initially contacts the floral surface.

If physical contact between a pollinator and a flower helps the pollinator find the floral resource of interest, then floral shape might play a significant role in mediating this final phase of

pollinator foraging. If that is the case, a deeper understanding of how flower morphology affects foraging performance can help elucidate the present ecology of both plant and pollinator.

The ability to explore the interaction of floral phenotype with pollinator behaviour is difficult in natural systems where genetic correlations among various floral traits may constrain the space of floral shape that can be explored. While it may be possible to create flowers of the desired phenotype through introgressive hybridization of natural populations, even under the most meticulous breeding program, some combinations of floral traits may be difficult or impossible to cultivate due to underlying developmental constraints. As a result, there has been a long tradition of fabricating artificial flowers of exactly the desired phenotype for testing in laboratory or controlled field experiments (Smith et al. 1996, Goyret & Raguso 2006, Sanderson et al 2006, Muchhala 2007, Yoshioka et al. 2007, Temeles et al. 2009, Whitney et al. 2009, Goyret 2010, Kaczoroski et al. 2012). But, with the advent of 3D printing technologies we have access to a powerful tool that can combine computer-aided design (CAD) with mathematical formulation to floral shape. That combination, in turn, can allow us to probe a much wider parameter space than could be made available by earlier fabrication methods or by natural breeding technologies. Thus, the combination of a natural pollinator with CAD-generated flowers presents a unique opportunity to explore the interactions between floral form and pollinator performance, essentially using high throughput technology for exploring the effects of floral morphological parameter space on pollinator foraging performance.

While real hawkmoth-pollinated flowers tend to have some degree of petal dissection and radial grooves leading toward the nectary, we modelled our artificial flowers as having no petal

dissection and no grooves. This was done to eliminate any possible contribution of these aspects of flower shape to nectar discovery ability since those variables were beyond the scope of our study and the positive effects of petal dissection and radial corolla grooves has already been demonstrated (Goyret & Raguso 2006).

## Materials and Methods

### Animals

Individuals of *M. sexta* were obtained from a colony maintained by the Department of Biology at the University of Washington, Seattle, WA, USA. Moths were allowed to eclose in indoor cages with a 12:12 light:dark cycle. Food-deprived, flower-naïve moths were used in experimental trials 2-5 days post-eclosion. We attempted to collect behavioural data from 70 moths for this study. Of those, 20 moths were excluded from the study because they failed to forage on the artificial flower array and 5 moths were excluded because they emptied all 16 flowers in the array in the allotted time, removing the ability to assess differences in foraging ability based on the metric of number of emptied flowers alone. This left a total of 45 moths from which data were analyzed for this study. Both male and female moths were used in this study (23 males and 22 females). No significant differences were found between the male and female data, so males and females were grouped for the final analysis.

**Construction of Artificial Flowers**

We designed artificial flowers with fused petals since this is typical of hawkmoth-pollinated flowers in nature. In designing our artificial flowers, we sought to do two things: quantify flower shape, which is often described in qualitative terms (tubular, trumpet-shaped, bell-shaped, funnelform, etc.); and distil the complexity of natural flower shape into a few key parameters that could be systematically and individually varied depending on the hypothesis under investigation. We devised a generalized shape equation that would allow us to control four aspects of floral shape: corolla curvature, nectary radius, flower length, and whole-flower radius (Fig. 2). Of these, only corolla curvature and nectary radius were manipulated in this study, but other floral shape parameters may be manipulated in future experiments. The shape equation is:

$$z(r) = L\left(\frac{r - r_0}{R}\right)^{e^c}$$

where $z$ represents the longitudinal axis of our flower model and $r$ represents the radial distance of the corolla from the central $z$-axis. In addition, $c$ is a curvature parameter determining the lateral profile of the corolla, $r_0$ is the nectary radius, $L$ is the flower length, and $R$ is the lateral extent of the corolla from edge of the nectary to the outer lip of the flower (note that whole-flower radius is equal to $r_0 + R$). This surface is then given an arbitrary thickness of 1 mm to create a volume. Finally, an adapter was designed at the bottom of the flower to allow a 200 $\mu$L PCR tube to be press-fitted onto the flower to act as a reservoir for artificial nectar (20% sucrose solution). The resulting three-dimensional volume was then fabricated in ABS plastic using a uPrint SE 3D printer. The ABS plastic used was white in color and effectively odorless. These flower models are rigid and do not flex or warp in response to subtle contact by *M. sexta* during

feeding. Five distinct flower morphologies were used in this study. The values of their shape parameters are shown in Table 1.

**Behavioral Assays**

Artificial flowers were placed in a 4 by 4 square array of 16 flowers with flower centres spaced 10 cm apart. A polystyrene foam box was used as the structural base for the flower array. The flower array was positioned so that the long axis of the flowers was orthogonal to the ground. The array was always dimorphic, populated by two distinct flower morphologies, present in equal numbers (8 of each). Flower position was randomized before each moth foraging trial. Each nectar reservoir was filled with 20 $\mu$L of 20% sucrose solution, which is typical of many hawkmoth-pollinated flowers (Raguso *et al*. 2003), and of lepidopteran-pollinated flowers in general (Watt et al 1974; Heinrich 1975; Kingsolver & Daniel 1979). The flower array was placed inside of a 90 x 90 x 65 cm (height x width x depth) glass-walled flight chamber. A white light LED array illuminated the flight chamber from above at an illuminance of 0.1 lux to simulate moonlight conditions. Illuminance was measured with a Gossen Mavolux 5032C lux meter at flower level on the centre of the flight chamber. The flight chamber was also illuminated with two bright infrared lights (Magnalight **LEDLB-16E-IR;** 790-880 nm flat emission peak) for recording foraging behaviours with an infrared video camera (Sony DCR-TRV310).

Moths were placed one at a time into the flight chamber and allowed to forage from the flower array for 5 minutes following the first visit to a flower. Each individual moth only took part in

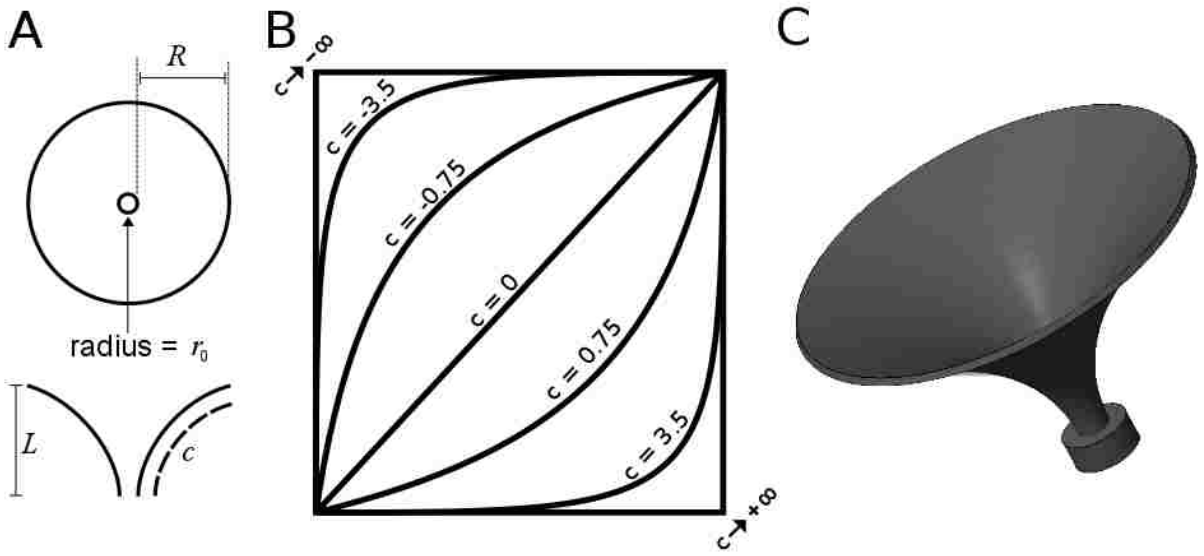


Figure 2.
(A) Bird's eye view (top) and lateral section (bottom) of generic artificial flower depicting what each of our four shape parameters represent. *R* is the linear distance between the nectary aperture edge and the edge of the "corolla" and $r_0$ is the radius of the central aperture. Note that this means that whole-flower radius is equal to $r_0 + R$. (B) Illustration showing how altering the value of the corolla curvature parameter, *c*, in our flower shape equation affects the lateral profile of our artificial flowers. When *c* is equal to 0, the corolla forms a straight line between the base of the flower and its outer lip, forming a truncated cone if revolved around the vertical axis. Negative values produce curved corolla profiles that lead to trumpet-shaped flowers if revolved around the vertical axis. As *c* approaches negative infinity, the corolla approaches a vertical path that turns suddenly at a 90-degree angle, producing a flat-disk flower with cylindrical nectar tube if revolved. Positive values of *c* produce bowl-shaped flowers if the resulting path is revolved. The given values of *c* are only for illustrating the trend. (C) A 3D computer rendering of what the flower in (A) would look like.

Table 1. Shape parameter values of the five artificial flower morphologies used in this study.

| Flower Morph | Length $L$ (mm) | Nectary radius $r_0$ (mm) | Corolla Lateral Extension $R$ (mm) | Curvature Parameter $c$ |
|---|---|---|---|---|
| M1 | 30 | 2.5 | 25 | −0.75 |
| M2 | 30 | 2.5 | 25 | $\rightarrow -\infty$ |
| M3 | 30 | 1.25 | 26.25 | −0.75 |
| M4 | 30 | 1.25 | 26.25 | $\rightarrow -\infty$ |
| M5 | 30 | 1.25 | 26.25 | −3.5 |

one foraging trial. Moths that did not take flight within 5 minutes of being placed in the flight chamber were replaced and not used again.

*Manduca sexta* requires olfactory cues to initiate its appetitive behaviour (Brantjes 1978; Goyret & Raguso 2006), so we placed a piece of filter paper impregnated with 8 μL of a 7-component mixture of floral scent inside of the flight chamber 5 minutes before the first foraging trial of a data collection session. The filter paper remained in the flight chamber between trials to keep the air in the chamber as saturated with scent as possible. This artificial flower scent is designed to be representative of a host of hawkmoth-pollinated flowers. Within a mineral oil vehicle, the floral scent mixture contained benzaldehyde (0.6%), benzyl alcohol (17.6%), and linalool (1.8%). These three compounds are sufficient to elicit behavioural responses similar to those elicited by natural *Datura wrightii* scent. *Manduca sexta* has an innate bias toward *D. wrightii* scent (Riffell et al. 2009b). The mixture also contained methyl salicylate (2.4%), nerol (3%), geraniol (9%), and methyl benzoate (0.6%), the latter being present in significant quantities in the headspace of many hawkmoth-pollinated flowers (Riffell et al. 2013).

After a foraging trial was completed, the moth was recaptured and the number of emptied flowers of each morph was recorded. Flowers were always either completely full or completely empty following a foraging trial, so the resulting data were composed of integer values ranging from 0 to 8 for each flower morph. Video of the foraging trials was also used to count the number of visits that the moths made to each flower morph.

For each of the three experiments described below, the sample size was equal at N = 15 foraging trials.

**Experiment 1**

In the first experiment, the two morphs present in the flower array were a trumpet-shaped morph (M1) and a flat-disk morph (M2) with 2.5 mm nectary radii. These two morphs will be referred to as M1 and M2 throughout the rest of this paper (Fig. 3; Table 1). Corolla curvature was the only difference between the two morphs. The design goal for these two morphs was to create a pair of flowers that differed markedly in their corolla curvature, with the flat-disk morph being putatively more difficult to exploit than the trumpet-shaped morph. The nectary radius of 2.5 mm was chosen so that we could be sure that nectary constriction was not a limiting factor to nectary discovery, as the proboscis of *M. sexta* is on the order of 1 mm wide. A flower length of 30 mm was chosen so as to ensure that moths could theoretically reach the nectary, their proboscis length ranging from 50-70 mm.

**Experiment 2**

The second experiment contained flower morphs that were identical to the flowers used in Experiment 1, except that nectary radius was reduced by half to 1.25 mm for both morphs (Fig. 3, M3 and M4). This is slightly larger than the nectary aperture sizes of *Datura wrightii* and *Petunia axillaris* (measured by us using digital callipers on one *D. wrightii* flower and six *P. axillaris* flowers taken opportunistically from the University of Washington greenhouse in February of 2014), two flowers that are visited by *M. sexta* in the wild (*D. wrightii* nectary radius: 1 mm; *P. axillaris* nectary radius mean: 0.7 mm ± 0.06 SEM).

**Experiment 3**

The third experiment again contained a flat-disk morph and a trumpet-shaped morph. The flat-disk morph was identical to the one used in Experiment 2 (Fig. 3, M4). The trumpet-shaped morph in this experiment had a corolla curvature such that it deviated from the flat-disk morph only slightly, having a sharp curve at the transition between the upper disk portion of the flower and the "nectar tube" portion of the flower instead of the exact 90-degree angle of the flat-disk morph (Fig. 3, M5).

**Statistical Analysis**

For each of our three experiments, we tested two null hypotheses: 1) the mean number of flowers of each morph that were emptied in the array is equivalent; and, 2) the mean number of visits to each flower morph in the array is equivalent. We used a series of permutation tests (Edgington 1969) to test these hypotheses. The data in each of our experiments took the form of two pairs of columns of numbers: the number of trumpet-shaped flowers with emptied nectaries and number of flat-disk flowers with emptied nectaries in each foraging trial; and the number of visits to each morph in each foraging trial. Under the null hypothesis, the difference between the means of each pair of columns should be zero. We used a custom MATLAB script to randomly permute (shuffle) the assignment of each data entry to the two categories (trumpet-shaped *vs*. flat-disk flowers) in the data table and then recalculate the difference between the means of the two permuted columns of data. The data were permuted 10,000 times and the resulting mean differences were used to construct the null sampling distribution against which the observed data were compared.

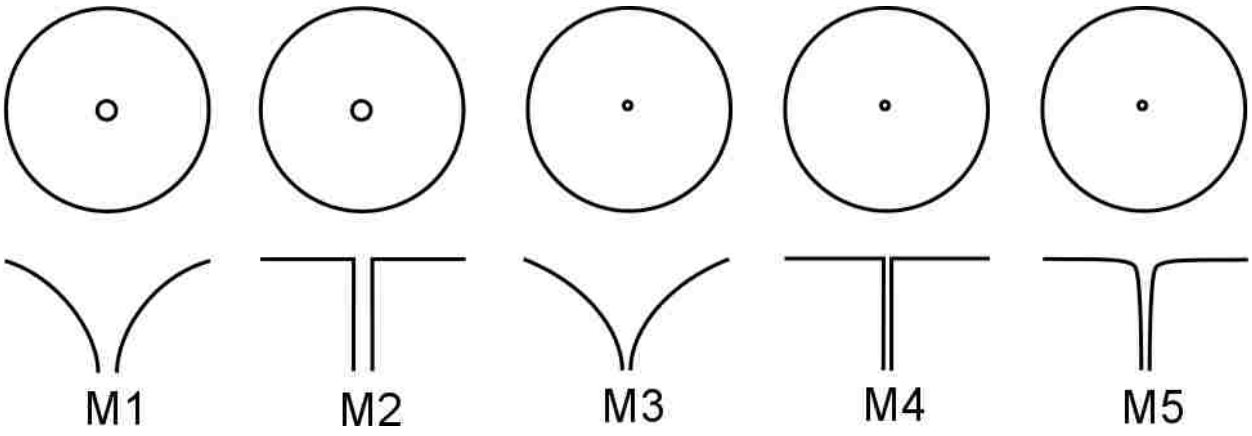


Figure 3.
Bird's eye view (top) and lateral section (bottom) of the five different artificial flower morphs used in our experiments. They are labeled M1 through M5 and referred to as such in the main text for convenience. All are drawn to the same scale.

Once our null sampling distributions were constructed, we performed 1-tailed tests of the null hypothesis by mapping our observed mean differences onto the corresponding sampling distributions and determining the fraction of the sampling distributions that rested between the observed mean difference and the end of the tail. This fraction is the 1-tailed *p*-value. We chose an α level of 0.05 for each of our individual tests.

## Results

In our first experiment comparing a trumpet-shaped flower against a flat-disk flower with 2.5 mm nectary radius, we found a significant difference in the number of emptied flowers, with trumpet-shaped flowers emptied more frequently than flat-disk flowers (Fig. 4A; M1 trumpet-shaped mean = 5.7 ± 0.57 SEM; M2 flat-disk mean = 3.9 7 ± 0.56 SEM; $p = 0.0443$). Moths did not show a tendency to visit one morph more than the other (M1 trumpet-shaped mean = 21.2 ± 2.9 SEM; M2 flat-disk mean = 19.2 7 ± 2.4 SEM; $p = 0.6134$) and did not exhibit constancy during foraging to a significant degree as measured by Bateman's index (Bateman 1951, and see also Waser 1986) (mean BI = -0.35 ± 0.10 SEM; $p > 0.99$). The subsequent two experiments were done with flower models with nectary radii reduced by half to 1.25, corresponding to a four-fold reduction in nectary size in terms of area. This reduction in nectary radius was the only difference between the flower models used in Experiment 1 and Experiment 2. With this one change, we saw an even greater difference in the number of emptied flowers of each morph (M3 trumpet-shaped mean = 7.6 ± 0.16 SEM; M4 flat-disk mean = 2.1 ± 0.44 SEM; $p < 0.0001$), but still no tendency to visit one morph more than the other (M3 trumpet-shaped mean = 31.9 ± 2.6 SEM; M4 flat-disk mean = 31.1 ± 3.3 SEM; $p = 0.4287$), and still no tendency towards constancy during foraging (mean BI = -0.09 ± 0.05 SEM; $p = 0.97$). In Experiment 3, we kept

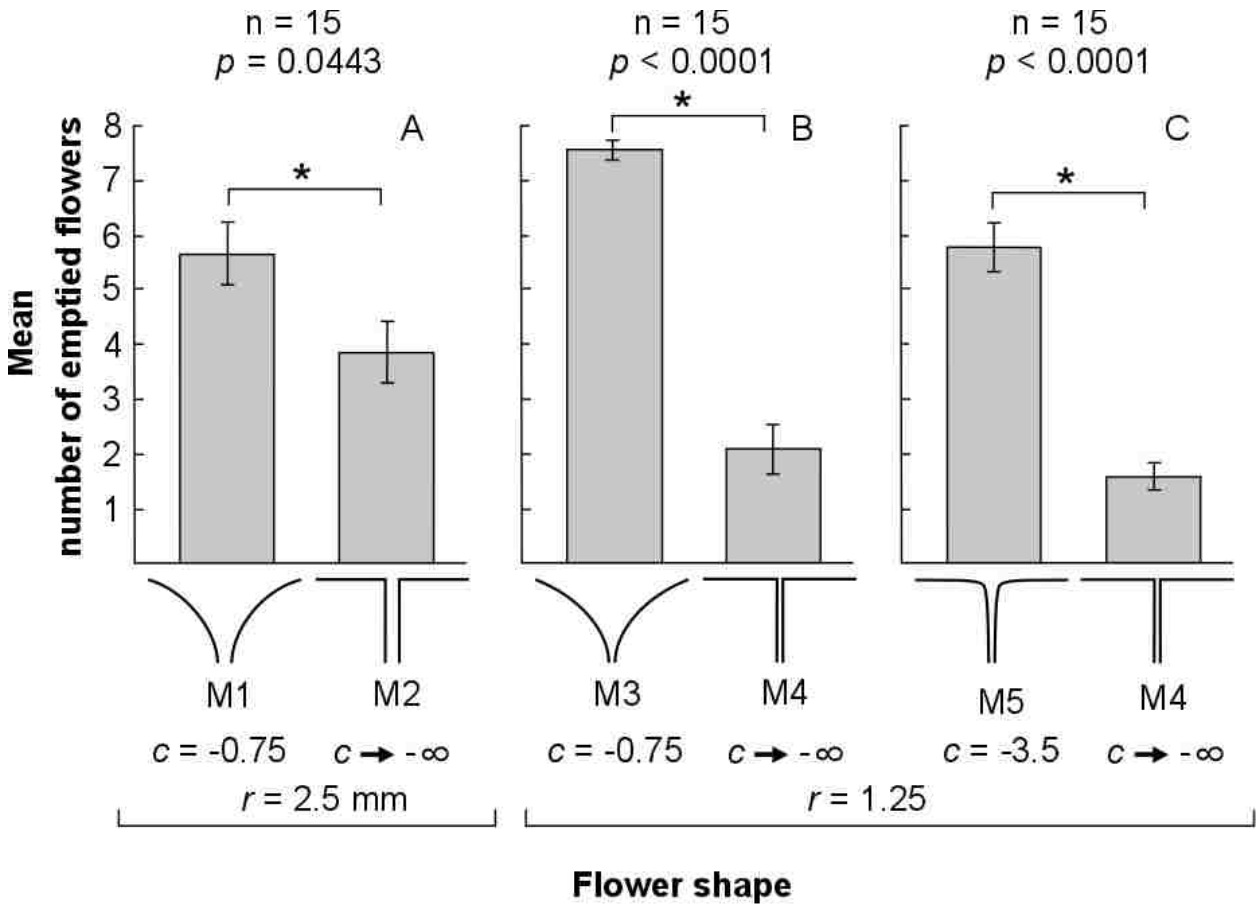


Figure 4.
Mean number of emptied flowers of each flower morph per foraging bout (± SEM) in each of our three experiments. Parts A-C correspond to Experiments 1-3 respectively. Significant differences are denoted with an asterisk.

the disk morph unchanged from the previous experiment but changed the curvature parameter of the trumpet-shaped morph so that it more closely approached the sharp 90-degree transition in lateral profile of the flat-disk morph. However, even with this change, we still saw the same pattern of flower exploitation heavily biased toward the curved trumpet-shaped flower (M5 trumpet mean = 5.8 ± 0.46 SEM; M4 flat-disk mean = 1.6 ± 0.25 SEM; $p < 0.0001$) and with no tendency to visit one morph more than the other (M5 trumpet mean = 26.7 ± 2.4 SEM; M4 flat-disk mean = 26.1 ± 2.5 SEM; $p = 0.4253$). Again, moths did not exhibit constancy during foraging during Experiment 3 (mean BI = -0.06 ± 0.03 SEM; $p = 0.79$).

## Discussion

We set out to test whether the centrally sloping morphology of trumpet-shaped flowers might act as a mechanical floral guide for the long proboscis of hawkmoths. Our results show that hawkmoths were indeed able to exploit trumpet-shaped flowers far better than flat-disk flowers in all three of our experiments (Fig. 4).

We excluded the possibility that this result could be due to an initial preference for either morph by showing that both flower morphs were visited with equal frequency and without constancy, supporting our hypothesis that the differences in foraging success were due to interactions between the moth's proboscis and the different tactile cues offered by trumpet-shaped and flat-disk flowers.

Krenn (1998) showed that the lepidopteran proboscis contains mechanoreceptors, especially at the proboscis tip where contact with a flower would initially be made. However, our data do not

allow us to discriminate between the alternatives of: 1) active mechanical sensing of a curved surface by *M. sexta via* the proboscis; and, 2) passive motion of the proboscis directed by the curved landscape of a trumpet-shaped corolla. This issue remains an open topic, particularly in the domain of sensory ecology where multiple sensory modalities mediate interactions between animals and plants.

Interestingly, moths presented with a flat-disk flower and a trumpet-shaped flower whose curvature was so slight that it qualitatively resemble the flat-disk morph to a high degree (Experiment 3) showed that even this small deviation from a flat-disk corolla towards the trumpet shape characteristic of hawkmoth-pollinated flowers is enough to significantly increase nectar discovery ability (Fig. 4C). Such sensitivity to slight curvature was unexpected and is indicative of the potential importance of corolla curvature as a mechanical floral guide. Future experiments will better define the strongly nonlinear relationship between corolla curvature and foraging success.

Results from others suggest that foraging by *M. sexta* is under multimodal sensory control, with different sensory modalities or combinations of them being important at different stages of the foraging process, depending on a moth's distance from a food source. At large distances, a moth uses olfaction to orient toward a group of flowers (Brantjes 1978). At intermediate distances, the approach to a group of flowers is guided by either olfaction or vision while extension of the proboscis requires that appropriate olfactory and visual stimuli be present simultaneously (Goyret et al. 2007). Once a moth has selected an individual flower, initial placement of the proboscis on the flower is visually guided, with lightly coloured regions being preferred over

dark regions (Goyret 2010). Finally, when the proboscis is in contact with the flower, mechanoreception through the proboscis ultimately is used to locate the nectar source (Goyret & Raguso 2006, Goyret 2010). Our results corroborate recent conclusions that *M. sexta* primarily uses tactile cues to find floral nectar during visits to individual flowers. However, while the experimental manipulations of Goyret & Raguso 2006 and Goyret 2010 focused on the role of floral surface features such as grooves, our results suggest that whole-flower shape might also function as a mechanical nectar guide for nocturnal/crepuscular moths foraging in low light.

We have shown that trumpet-shaped corolla curvature assists moths in exploiting floral resources. But this phenotypic feature might also facilitate pollination for the flower by helping to align the animal with the flower's reproductive parts. If, for example, the anthers and stigma are located along the centre-line of the flower, then the trumpet shape could force a visiting animal toward the reproductive parts while still allowing sufficient access to the reward. In that case, the -3.5 curvature flower (Fig. 4C) flower could have been pollinated more, and consequently would have been more fit, than the -0.75 flowers (Fig. 4A-B). Flower petals have indeed been shown to act as positioners for hummingbirds, facilitating pollen deposition (Temeles and Rankin 2000). Given this, why do many night-blooming flowers qualitatively resemble the -0.75 corolla curvature? One explanation is that corolla curvature could be under balancing selection due to interactions with other animal species, pollinator or otherwise, as in the finding that phenotypic variation in flower form in the alpine wildflower *Polemonium viscosum* was maintained by conflicting demands for pollinator attraction and enemy avoidance (Galen 1999).

It is important to note that there is increasing evidence that nectarivory is influenced not only by the host of floral morphological parameters mentioned above, but also by the dynamics of floral motion (Sprayberry & Daniel 2007). Thus the ability of a moth to exploit a flower depends as well upon how effectively it can track a moving flower. That tracking could depend upon both the visual tracking capability of a pollinator and upon any mechanosensory signals (at the level of the proboscis) they may process. Both sensory stimuli are potentially influenced by floral shape. Thus while Sprayberry and Daniel (2007) showed that motion and morphology combine to determine pollinator foraging success there are a host of open topics that include the roles of luminance, mechanosensing, and even the frequency characteristics of the natural motions of flowers.

As mentioned previously, we did not need to manipulate all of the floral shape parameters in our generalized shape equation in order to test the hypotheses presented in this paper. Many different experiments investigating the role of floral form in determining pollinator foraging effectiveness are still possible. In particular, nectary width and length are known to be important determinants of pollination success in Malagasy long-spurred orchids (Nilsson et al. 1985, Nilsson 1988). Our ability to manipulate mathematically-specified artificial flower morphology means that we have the ability to investigate the role of minute but potentially important differences in floral form on pollinator foraging performance, independent of evolutionary and developmental constraints on the shape of flowers in nature. Furthermore, additional floral features such as separated petals, bilateral symmetry, and rotation of the corolla along the long axis of a flower are all possible *via* the addition of more parameters to the shape equation. We

hope that such precise, well-defined, reproducible flower construction techniques can open the door to otherwise inaccessible or difficult manipulations of floral form.

Using the power of computer-aided design and rapid prototyping technologies, it is increasingly possible to explore how individual aspects of floral morphology influence plant-pollinator interactions. These interactions, mediated by physical contact between the flower and the animal, are a major determinant in the effectiveness with which pollen is transferred to conspecific flowers. Using the methods and 3D-printing technologies in this study, it is possible to construct not only foraging performance landscapes as a function of variation in flower morphology, but also flower fitness landscapes as pollinators attempt to forage from populations of computationally-derived floral forms. Such studies can help elucidate the details of how pollinator visitation influences the evolution of floral shape in nature, and the extent to which floral forms are the result of specializations between one plant and one pollinator species, or generalization due to multiple species of visitors exerting significant but non-similar selective pressures.

## Acknowledgments

This work benefited greatly from careful reading and suggestions from members of the Daniel Lab and Bradshaw Lab, as well as from Marie Clifford and Ellie Theobald. Thanks to Jeff Riffell for the supply of artificial flower scent. Janneke Hille Ris Lambers and Joe Felsenstein provided advice on the statistical analysis. Comments from two anonymous reviewers also greatly improved this work. Financial support was provided by the Komen Endowed Chair to TLD, Office of Naval Research Grant N00014-01-1-0676 to TLD, and a National Institutes of

Health grant to HDB (5R01GM088805). This study is based upon work supported by the National Science Foundation Graduate Research Fellowship under Grant No. DGE-0718124 to EOC. This material was also supported by a Bank of America Endowed Fellowship from the University of Washington Graduate School, through the Graduate Opportunities & Minority Achievement Program (GO-MAP), to EOC. I declare no conflicts of interest associated with this work.

## Data Accessibility

Data are deposited in the University of Washington Research Works Archive.

http://hdl.handle.net/1773/27082 (Campos, Bradshaw & Daniel 2015).

## References

Bateman, A.J. (1951) The taxonomic discrimination of bees. *Heredity*, **5**, 271-278.

Brantjes, N.B.M. (1978) Sensory responses to flowers in night-flying moths. *The Pollination of Flowers by Insects* (ed. A. J. Richards), pp. 13-19. Academic Press, London.

Brantjes, N.B.M. & Bos, J.J. (1980) Hawkmoth behavior and flower adaptation reducing self pollination in two Liliflorae. *New Phytologist*, **84**, 139-143.

Dar, S., Arizmendi, M.D. & Valiente-Banuet, A. (2006) Diurnal and nocturnal pollination of *Marginatocereus marginatus* (Pachycereeae: Cactaceae) in Central Mexico. Annals of Botany, 97, 423-427.

Edgington, E.S. (1969) Approximate randomization tests. *Journal of Psychology*, **72**,143-149.

Fægri K. & van der Pijl, L. (1966) *The Principles of Pollination Ecology*. Pergamon Press, Toronto, New York.

Galen, C. (1999) Flowers and enemies: predation by nectar-thieving ants in relation to variation in floral form of an alpine wildflower, *Polemonium viscosum*. *Oikos*, **85**, 526-434.

Goyret, J. (2010) Look and touch: multimodal sensory control of flower inspection movements in the nocturnal hawkmoth *Manduca sexta*. *Journal of Experimental Biology*, **213**, 3676–3682.

Goyret, J. & Kelber, A. (2011) How does a diurnal hawkmoth find nectar? Differences in sensory control with a nocturnal relative. *Behavioral Ecology*, **22**, 976-984.

Goyret, J., Markwell, P.M, & Raguso R.A. (2010) The effects of decoupling olfactory and visual stimuli on the foraging behavior of Manduca sexta. *Journal of Experimental Biology*, **210**, 1398-1405.

Goyret, J. & Raguso, R.A. (2006) The role of mechanosensory input in flower handling efficiency and learning by *Manduca sexta*. *Journal of Experimental Biology*, **209**, 1585–1593.

Groman, J.D. & Pellmyr, O. (1999) The pollination biology of *Manfreda virginica* (Agavaceae): relative contribution of diurnal and nocturnal visitors. *OIKOS*, **87**, 373-381.

Heinrich, B. (1975) Energetics of Pollination. *Annual Reviews of Ecology and Systematics*, **6**, 139-170.

Kaczorowski, R.L., Seliger, A.R., Gaskett, A.C., Wigsten, S.K., & Raguso, R.A. (2012) Corolla shape vs. size in flower choice by a nocturnal hawkmoth pollinator. *Functional Ecology*, **26**, 577-587.

Kevan, P.G. & Lane, M.A. (1985) Flower petal microtexture is a tactile cure for bees. *Proceeding s of the National Academy of Sciences of the United States of America*, **82**, 4750-4752.

Kingsolver, J.G. & Daneil, T.L. (1979) Mechanics and energetics of nectar feeding in butterflies. *Journal of Theoretical Biology*, **76**, 167-179.

Kingsolver, J.G. & Daneil, T.L. (1995) Mechanics of food handling by fluid-feeding insects. *Regulatory Mechanisms in Insect Feeding*. (ed. R.F. Chapman and G. de Boer), pp. 32-73. Chapman & Hall, New York.

Krenn, H.W. (1998) Proboscis sensilla in *Vanessa cardui* (Nymphalidae, Lepidoptera): functional morphology and significance in flower probing. *Zoomorphology*, **118**, 23-30.

Medel, R., Botto-Mahan, C. & Kalin-Arroyo, M. (2003) Pollinator-mediated selection on the nectar guide phenotype in the Andean monkey flower, *Mimulus luteus*. *Ecology*, **84**, 1721-1732.

Muchhala, N. (2007) Adaptive trade-off in floral morphology mediates specialization for flowers pollinated by bats and humminbirds. *The American Naturalist*, **169**, 497-504.

Nilsson, L.A., Jonsson, L., Rason, L. & Randrianjohany, E. (1985) Monophily and pollination mechanisms in *Angraecum arachnites* Schltr. (Orchidaceae) in a guild of long-tongued hawk-moths (Sphingidae) in Madagascar. *Biological Journal of the Linnean Society*, **26**, 1-19.

Nilsson, L.A. (1988) The evolution of flowers with deep corolla tubes. *Nature*, **334**, 147-149.

Norberg, U.M. (1990) *Vertebrate Flight: Mechanics, Physiology, Morphology, Ecology, and Evolution*. Springer-Verlag, Berlin.

Proctor, M., Yeo, P. & Lack, A. (1996) *The natural history of pollination*. HarperCollins, London.

Raguso, R.A. & Willis, M.A. (2002) Synergy between visual and olfactory cues in nectar feeding by naïve hawkmoths, *Manduca sexta*. *Animal Behaviour*, **64**, 685-695.

Raguso, R.A., Henzel, C., Buchmann, S.L. & Nabhan, G.P. (2003) Trumpet flowers of the Sonoran Desert: floral biology of *Peniocereus* cacti and Sacred *Datura*. *International Journal of Plant Sciences*, 1**64**, 877-892.

Riffell, J.A., Lei, H., Abrell, L. & Hildebrand, J.G. (2013) Neural basis of a pollinator's buffet: Olfactory specialization and learning in *Manduca sexta*. *Science*, **339**, 200-204.

Riffell, J.A., Lei, H., Christensen, T.H. & Hildebrand, J.G. (2009) Characterization adn coding of behaviorally significant odor mixtures. *Current Biology*, **19**, 335-340.

Riffell, J.A., Lei, H. & Hildebrand, J.G. (2009) Neural correlates of behavior in the moth *Manduca sexta* in response to complex odors. *Proceedings of the National Academy of the Unites States of America*, **106**, 19219-19226.

Sanderson, C.E., Orozco, B.S., Hill, P.S.M, & Wells, H. (2006) Honeybee (Apis mellifera ligustica) response to differences in handling time, rewards and flower colours. *Ethology*, **112**, 937-946.

Smith, C.E., Stevens, J.T., Temeles, E.J., Ewald, P.W., Hebert, R.J., & Bonkovsky, R.L. (1996) Effects of floral orifice width and shape on hummingbird-flower interactions. *Oecologia*, **106**, 482-492.

Sprayberry, J.D.H. & Daniel, T.L. (2007) Flower tracking in hawkmoths: Behavior and energetics. *Journal of Experimental Biology*, **210**, 37-45.

Sprengel, C.K. (1793) *Das endtdeckte Geheimnis der Natur im Bau und in der Befruchtung der Blemen*. F. Vieweg, Berlin.

Sprengel, C.K. (1996) Discovery of the secret of nature in the fertilization of flowers. *Floral Biology: Studies on Floral Evolutin in Animal-Pollinated Plants* (ed. D.G. Lloyd, S.C.H. Barrett), pp. 3-43. Chapman & Hall, New York.

Temeles, E.J., Koulauris, C.R., Sander, S.E., & Kress, W.J. (2009) Effect of flower shape and size on foraging performance and trade-offs in a tropical hummingbird. *Ecology*, **90**, 1147-1161.

Temeles, E.J. & Rankin, A.G. (2000) Effects of the lower lip of *Monarda didyma* on pollen

removal by hummingbirds. *Canadian Journal of Botany*, **78**, 1164-1168.

Vogel, S. (1994) *Life in moving fluids*. Princeton University Press, Princeton.

Waser, N.M. (1986) Flower constancy: definition, cause, and measurement. *The American Naturalist*, **127**, 593-603.

Watt, W.B, Hoch, P.C. & Mills, S.G. (1974) Nectar resource use by *Colias* butterflies – Chemical and visual aspects. *Oecologia*, **14**, 353-374.

Whitney, H.M., Chittka, L., Bruce, T.J.A., & Glover, B.J. (2009) Conical epidermal cells allow bees to grip flowers and increase foraging efficiency. *Current Biology*, **19**, 948-953.

Yoshioka, Y., Ohashi, K., Konuma, A., Iwata, H., Ohsawa, R., & Ninomiya, S. (2007) Ability of bumblebees to discriminate differences in the shape of artificial flowers of *Primula sieboldii* (Primulaceae). *Annals of Botany*, **99**, 1175-1182.

Appendix

# CODE LISTING

## *A.1 Mathematical modeling of flower shape*

This MATLAB code is for exploring artificial flower shape parameter space. This script has its text soft-wrapped.

```
% This code generates graphs representing simplified "flower" structures
% using three shape parameters: width, height, and curvature
% ====================
% (Block 1)
% This block prompts user input in the Command Window for (hopefully)
% easier manual exploration of parameter space
%
% PetalWidth = input('Flower Petal Width (positive numbers only): ');
% Height = input('Flower Height (positive numbers only): ');
% Curvature = input('Curvature Parameter (positive or negative numbers ok):
'); % negative values give trumpet shape; 0 gives cone; positive values give
bowl shape
% CentralRadius = input('Central Radius (positive numbers only): ');
% RotationSteps = input('Number of rotation steps (slices) to execute: ');
% ConcentricSteps = input('Number of concentric steps (rings) to execute: ');
% Thickness = input('Thickness of flower surface: '); % approximate distance
between inner and outer "shells" (surfaces)
% disp(' ');
% ====================
% (Block 2)
PetalWidth = 26.25;
Height = 30;
Curvature = -1.5; % negative values give trumpet shape; 0 gives cone;
positive values give bowl shape
CentralRadius = 1.25;
RotationSteps = 12;
ConcentricSteps = 20; % set to 20 for nice results
Thickness = 0.1; % approximate distance between inner and outer "shells"
(surfaces)
% Make sure that either the coding regions of Block 1 or Block 2 are
commented out before executing
% ====================
theta = 0:(2*pi)/RotationSteps:2*pi;
% Main shell (or inner surface)
r = (CentralRadius:(PetalWidth)/ConcentricSteps:PetalWidth+CentralRadius);
z = (Height*(((1/PetalWidth)*(r-CentralRadius)).^((exp(1)).^Curvature)));
%
xx = bsxfun(@times,r',cos(theta));
yy = bsxfun(@times,r',sin(theta));
zz = repmat(z',1,length(theta));

% ====================
% Outer shell (or surface)
r_2 =
(CentralRadius+Thickness:(PetalWidth)/ConcentricSteps:PetalWidth+CentralRadiu
```

```
s+Thickness);
z_2 = (-Thickness)+(Height*(((1/PetalWidth)*(r-
CentralRadius)).^((exp(1)).^Curvature)));
%
xx_2 = bsxfun(@times,r_2',cos(theta));
yy_2 = bsxfun(@times,r_2',sin(theta));
zz_2 = repmat(z_2',1,length(theta));

% create upper curtain
r_upper_curtain =
(PetalWidth+CentralRadius):Thickness:(PetalWidth+CentralRadius+Thickness);
z_upper_curtain = Height+(-(r_upper_curtain-(PetalWidth+CentralRadius)));
xx_upper_curtain = bsxfun(@times,r_upper_curtain',cos(theta));
yy_upper_curtain = bsxfun(@times,r_upper_curtain',sin(theta));
zz_upper_curtain = repmat(z_upper_curtain',1,length(theta));

% r_upper_curtain = 4:3:7;
% z_upper_curtain = -r_upper_curtain;
% xx_upper_curtain = bsxfun(@times,r_upper_curtain',cos(theta));
% yy_upper_curtain = bsxfun(@times,r_upper_curtain',sin(theta));
% zz_upper_curtain = repmat(z_upper_curtain',1,length(theta));

% Create lower curtain
r_lower_curtain = CentralRadius:Thickness:CentralRadius+Thickness;
z_lower_curtain = -(r_lower_curtain-CentralRadius);
xx_lower_curtain = bsxfun(@times,r_lower_curtain',cos(theta));
yy_lower_curtain = bsxfun(@times,r_lower_curtain',sin(theta));
zz_lower_curtain = repmat(z_lower_curtain',1,length(theta));

% %Add inner, top ring to outer shell:
% xx_2 = [xx_2;xx(size(xx,1),:)];
% yy_2 = [yy_2;yy(size(yy,1),:)];
% zz_2 = [zz_2;zz(size(zz,1),:)];
%
% %Add outer, bottom ring to inner shell:
% xx = [xx_2(1,:);xx];
% yy = [yy_2(1,:);yy];
% zz = [zz_2(1,:);zz];


% ====================
% Reshapes the above matrices into single columns of coordinates:
% x_column = reshape(xx,(RotationSteps+1)*(ConcentricSteps+2),1);
% y_column = reshape(yy,(RotationSteps+1)*(ConcentricSteps+2),1);
% z_column = reshape(zz,(RotationSteps+1)*(ConcentricSteps+2),1);
% ====================
% Reshapes the above matrices into single columns of coordinates:
% x_column_2 = reshape(xx_2,(RotationSteps+1)*(ConcentricSteps+2),1);
% y_column_2 = reshape(yy_2,(RotationSteps+1)*(ConcentricSteps+2),1);
% z_column_2 = reshape(zz_2,(RotationSteps+1)*(ConcentricSteps+2),1);
% ====================


% Vertically concatenates the columns from each shell along each axis:
% total_x_column = [x_column; x_column_2];
```

```
% total_y_column = [y_column; y_column_2];
% total_z_column = [z_column; z_column_2];
% ====================
% Concatenates the three columns above into an x,y,z matrix:
% concat_matrix = horzcat(total_x_column,total_y_column,total_z_column);
% ====================


% plots the two surfaces to get an idea of the final "thickness" of the
object:
figure(1)
surf(xx,yy,zz)
hold on
surf(xx_2,yy_2,zz_2)
surf(xx_upper_curtain,yy_upper_curtain,zz_upper_curtain)
surf(xx_lower_curtain,yy_lower_curtain,zz_lower_curtain)
view(90,0)
axis equal
hold off

% ====================
% plots a single surface:
% figure (2)
% surf(xx,yy,zz)
% axis equal
% ====================
% plots the point cloud of the two surfaces:
% figure(3)
% scatter3(total_x_column,total_y_column,total_z_column,10,'o','filled')
% axis equal
% figure(4)
% surf(xx_upper_curtain,yy_upper_curtain,zz_upper_curtain)
% hold on
% surf(xx_lower_curtain,yy_lower_curtain,zz_lower_curtain)
% axis equal
% hold off

figure(5)
plot(r,z)
axis equal

% end of script
```

### *A.2 Random artificial flower shuffling for behavioral experiments*

This Python code does as described above, for a 16-flower 4x4 square array. This script is soft-wrapped here.

```
# Written for Python 2.7
import random
ArrayFlowers01 = ["curved_1", "curved_2", "curved_3", "curved_4", "curved_5",
"curved_6", "curved_7", "curved_8", "flat___1", "flat___2", "flat___3",
"flat___4", "flat___5", "flat___6", "flat___7", "flat___8"]
```

```
ArrayFlowers02 = ["curved_1", "curved_2", "curved_3", "curved_4", "curved_5",
"curved_6", "curved_7", "curved_8", "flat___1", "flat___2", "flat___3",
"flat___4", "flat___5", "flat___6", "flat___7", "flat___8"]
ArrayFlowers03 = ["curved_1", "curved_2", "curved_3", "curved_4", "curved_5",
"curved_6", "curved_7", "curved_8", "flat___1", "flat___2", "flat___3",
"flat___4", "flat___5", "flat___6", "flat___7", "flat___8"]
ArrayFlowers04 = ["curved_1", "curved_2", "curved_3", "curved_4", "curved_5",
"curved_6", "curved_7", "curved_8", "flat___1", "flat___2", "flat___3",
"flat___4", "flat___5", "flat___6", "flat___7", "flat___8"]
ArrayFlowers05 = ["curved_1", "curved_2", "curved_3", "curved_4", "curved_5",
"curved_6", "curved_7", "curved_8", "flat___1", "flat___2", "flat___3",
"flat___4", "flat___5", "flat___6", "flat___7", "flat___8"]
ArrayFlowers06 = ["curved_1", "curved_2", "curved_3", "curved_4", "curved_5",
"curved_6", "curved_7", "curved_8", "flat___1", "flat___2", "flat___3",
"flat___4", "flat___5", "flat___6", "flat___7", "flat___8"]
ArrayFlowers07 = ["curved_1", "curved_2", "curved_3", "curved_4", "curved_5",
"curved_6", "curved_7", "curved_8", "flat___1", "flat___2", "flat___3",
"flat___4", "flat___5", "flat___6", "flat___7", "flat___8"]
ArrayFlowers08 = ["curved_1", "curved_2", "curved_3", "curved_4", "curved_5",
"curved_6", "curved_7", "curved_8", "flat___1", "flat___2", "flat___3",
"flat___4", "flat___5", "flat___6", "flat___7", "flat___8"]
ArrayFlowers09 = ["curved_1", "curved_2", "curved_3", "curved_4", "curved_5",
"curved_6", "curved_7", "curved_8", "flat___1", "flat___2", "flat___3",
"flat___4", "flat___5", "flat___6", "flat___7", "flat___8"]
ArrayFlowers10 = ["curved_1", "curved_2", "curved_3", "curved_4", "curved_5",
"curved_6", "curved_7", "curved_8", "flat___1", "flat___2", "flat___3",
"flat___4", "flat___5", "flat___6", "flat___7", "flat___8"]

random.shuffle(ArrayFlowers01)
random.shuffle(ArrayFlowers02)
random.shuffle(ArrayFlowers03)
random.shuffle(ArrayFlowers04)
random.shuffle(ArrayFlowers05)
random.shuffle(ArrayFlowers06)
random.shuffle(ArrayFlowers07)
random.shuffle(ArrayFlowers08)
random.shuffle(ArrayFlowers09)
random.shuffle(ArrayFlowers10)

print
print "A1"
for shape in ArrayFlowers01:
    if ArrayFlowers01.index(shape) + 1 < 10:
        print "", ArrayFlowers01.index(shape) + 1, shape
    else:
        print ArrayFlowers01.index(shape) + 1, shape

print
print "A2"
for shape in ArrayFlowers02:
    if ArrayFlowers02.index(shape) + 1 < 10:
        print "", ArrayFlowers02.index(shape) + 1, shape
    else:
        print ArrayFlowers02.index(shape) + 1, shape
```

```
print
print "A3"
for shape in ArrayFlowers03:
    if ArrayFlowers03.index(shape) + 1 < 10:
        print "", ArrayFlowers03.index(shape) + 1, shape
    else:
        print ArrayFlowers03.index(shape) + 1, shape

print
print "A4"
for shape in ArrayFlowers04:
    if ArrayFlowers04.index(shape) + 1 < 10:
        print "", ArrayFlowers04.index(shape) + 1, shape
    else:
        print ArrayFlowers04.index(shape) + 1, shape

print
print "A5"
for shape in ArrayFlowers05:
    if ArrayFlowers05.index(shape) + 1 < 10:
        print "", ArrayFlowers05.index(shape) + 1, shape
    else:
        print ArrayFlowers05.index(shape) + 1, shape

print
print "A6"
for shape in ArrayFlowers06:
    if ArrayFlowers06.index(shape) + 1 < 10:
        print "", ArrayFlowers06.index(shape) + 1, shape
    else:
        print ArrayFlowers06.index(shape) + 1, shape

print
print "A7"
for shape in ArrayFlowers07:
    if ArrayFlowers07.index(shape) + 1 < 10:
        print "", ArrayFlowers07.index(shape) + 1, shape
    else:
        print ArrayFlowers07.index(shape) + 1, shape

print
print "A8"
for shape in ArrayFlowers08:
    if ArrayFlowers08.index(shape) + 1 < 10:
        print "", ArrayFlowers08.index(shape) + 1, shape
    else:
        print ArrayFlowers08.index(shape) + 1, shape

print
print "A9"
for shape in ArrayFlowers09:
    if ArrayFlowers09.index(shape) + 1 < 10:
        print "", ArrayFlowers09.index(shape) + 1, shape
    else:
        print ArrayFlowers09.index(shape) + 1, shape
```

```
print
print "A10"
for shape in ArrayFlowers10:
    if ArrayFlowers10.index(shape) + 1 < 10:
        print "", ArrayFlowers10.index(shape) + 1, shape
    else:
        print ArrayFlowers10.index(shape) + 1, shape
# end script
```

### *A.3 Custom software implementation of permutation test*

This MATLAB code performs a permutation test to address the null hypothesis that the means of two groups are not different from each other. Permutation tests were used instead of t-tests in my statistical analyses. Permutation tests have an advantage over t-tests in that permutation tests allow you to construct the sampling distribution that will be used to calculate a p-value from empirical data, instead of relying on the assumption that a t-distribution accurately represents the sampling distribution from which the empirical data were drawn. This script is soft-wrapped here:

```
% first half of all_data is number of curved flowers emptied; second half
% is number of flat flowers emptied
all_data = [8
7
3
2
2
7
8
7
8
8
4
5
4
5
7
7
1
3
1
0
5
5
5
3
5
2
6
3
6
6];
```

```
% curved minus flat:
actual_diffs = zeros(length(all_data)/2,1);
for i = 1:length(actual_diffs)
    actual_diffs(i) = all_data(i)-all_data(i+length(actual_diffs));
end

actual_mean = mean(actual_diffs);

% ======================

indexed_data = zeros(length(all_data),2);
indexed_data(:,1) = 1:1:length(all_data);
indexed_data(:,2) = all_data;

indexed_perm_data = indexed_data;

permuted_data = zeros(length(all_data),2);

diffs = zeros(length(all_data)/2,1);

stored_means = zeros(10000,1);

stored_shuffled_data = zeros(length(all_data),10000);

tic

for j = 1:10000

    permutation = randperm(length(all_data));

    permuted_data(:,1) = permutation;

    for k = 1:length(all_data)
        permuted_data(k,2) = all_data(permutation(k));
    end

    for k = 1:length(diffs)
        diffs(k) = permuted_data(k,2)-permuted_data(k+length(diffs),2);
    end

    mean_of_diffs = mean(diffs);

    stored_shuffled_data(:,j) = permuted_data(:,2);

    stored_means(j) = mean_of_diffs;
end

sorted_stored_means = sort(stored_means);

toc

figure(1), hist(stored_means,100)
bins = hist(stored_means,100);
```